OWL PHASE A STATUS REPORT

P. Dierickx, E. Brunetto, F. Comeron, R. Gilmozzi, F. Gonte, F. Koch,
M. le Louarn, G. Monnet, J. Spyromilio, I. Surdej, C. Verinaud, N. Yaitskova

European Southern Observatory

ABSTRACT

Progress in the conceptual design phase of ESO's OWL 100-m optical and near-infrared telescope is reported, with emphasis on the development of the science case. The Phase A opto-mechanical design is now basically completed, and provides a clean, symmetrical geometry of the pupil, with a near-circular outer edge. We also report about the latest outcome of industrial studies, introduce the essential definition of the wavefront control systems, and outline operational concepts and instruments priorities. Finally, we elaborate on the favorable cost factors associated to the telescope design, its compatibility with low industrial risks, and argue that progressive implementation allows for competitive timescales. In particular, we show that suitable fabrication and integration schemes should accommodate for a start of science operation at unequalled potential and within a time frame comparable to that of smaller designs, while at the same time maximizing R&D time for critical subsystems.

Keywords: Extremely Large Telescopes, OWL, segments fabrication, wavefront control, science objectives

1. INTRODUCTION

A notional concept of the 100-m class OWL optical and near-infrared telescope was laid down in 1998 [1], in response to complementary science objectives mainly driven by HST and JWST. As of today, OWL's design nears phase A maturity, with an opto-mechanical design supported by extensive trade-offs and analysis. Under ESO contract, industrial studies have confirmed the timely feasibility and affordability of the concept. Further studies, including but not limited to enclosure, operation and maintenance infrastructures, will be contracted prior to the conceptual design review, scheduled by end-2005.

Optical fabrication of the segments has been addressed *in extenso* under contract with suppliers: production of the segment blanks and their optical figuring, in three optional segment's sizes (1.3, 1.8 and 2.3-m flat-to-flat) and different materials (classical glass-ceramics e.g. SCHOTT Zerodur™ and LZOS Astro-Sital™, as well as silicon carbide by Boostec and ECM). Owing to the reliance of OWL on proven industrial processes, all studies so far gave remarkably consistent results as to cost and schedule estimates, broadly in-line with initial expectations. The industrial capacity required to supply about one finished segment per day is somewhat better than expected, at a cost compatible with initial estimates, within manageable and known risks, and without implying unreasonable capital investment.

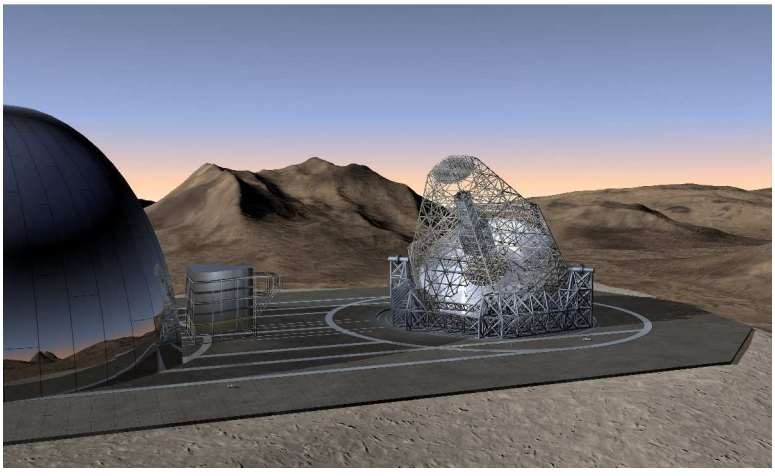

Fig. 1. Layout of the OWL facilities.

The design of the telescope structure and kinematics is arguably beyond what one would normally expect from a conceptual design phase, with a consolidated concept supported by extensive analysis

and fabrication studies. The modular design relies extensively on standard or serially produced parts, allowing for flexible, fast supply and integration lines.

Pupil size (diameter)	100	m
Collecting area	> 6000	m2
Multi-conjugate Adaptive Optics		
Diffraction-limited field of view :		
Visible (0.5 μm)	> 30	arc sec.
Infrared (2 μm)	> 2	arc min.
Strehl ratio (at 0.5 μm)		
Requirement	20	%
Goal	30	%
Seeing-limited field of view	10	arc min.
Wavelength range	0.32-12	μm
Elevation range		
Operational	30-89	degrees
Technical	0-90	degrees
Max. cost (capital investment)	1000	M€

Table 1. Overall design characteristics

Extensive effort has been put into the development of a suitable phasing metrology by European research organizations [2,3,4], with concepts now moving to the laboratory prior to testing on-sky [11] testing. Computational Fluid Dynamics (CFD) simulations have been performed to evaluate the performance of the design under wind load, and derive specifications of the control systems. The design being far less sensitive to decenters than classical Ritchey-Chrétien solutions, the main issue is the effect of wind on high spatial frequency inter-segments displacements. While CFD simulations seem to provide realistic results at low frequencies –below ~0.5 Hz, they are suspected to provide grossly optimistic high frequency pressure distributions. A measurement campaign has been initiated, an array of pressure sensors being currently installed on the Jodrell Bank 70-m radio-telescope in Manchester. Wind tunnel testing is also in preparation. Backup design options have been identified to alleviate the adverse effect of wind, if required.

A detailed implementation plan has been elaborated under the assumption that ESO would proceed with a detailed design phase over the period 2006-2010, with construction essentially ramping up at the time of ALMA completion. This plan assumes gradual implementation of adaptive optics, progressive filling of the aperture, and incorporates generous allocations for the development of critical technologies, setting up and debugging of the necessary control loops. A faster schedule is almost certainly possible, subject to early funding. The incompressible part is the supply of two 8-m class active mirrors, estimated at 6 years on the basis of VLT experience.

2. SCIENCE OBJECTIVES

A 100-m telescope working at the diffraction limit (e.g. 1 mill-arcsecond at V ~ 37) has an unprecedented scientific potential (not least for new discoveries). In contrast, a seeing-limited 100-m telescope (deprecatingly named a "light-bucket") would probably be scientifically unjustified. Discussion on science cases in the framework of the OPTICON working group on science with Extremely Large Telescopes (ELTs) can be found elsewhere [20]. Here we summarize some recently developed cases for OWL, in particular those that take full advantage of its capabilities: the spectroscopy of exo-earths to look for signs of life, and some of the cosmological science cases.

Spectroscopy of earth-like exoplanets. Searching for exo-biospheres could be defined as the *holy grail* of today's astronomy. This science case depends very strongly on the telescope diameter. First of all, the volume accessible to a telescope is proportional to D^3 (since resolution is $\propto D$). For example, the number of accessible G stars in the solar neighbourhood where an earth at 1 AU could be detected would be 20, 165 and 750 respectively for a 30-, 50- and 100-m telescope (assuming minimum resolvable separation $5\lambda/D$). From the point of view of the sensitivity, the time to achieve the same S/N in the planet (for objects in common, of course) is $\propto D^4$ (the planet is $\sim 10^{10}$ times fainter than the parent star, and even at many λ/D from the star we are definitely in the background-limited regime). This means that a 30-m telescope would need ~

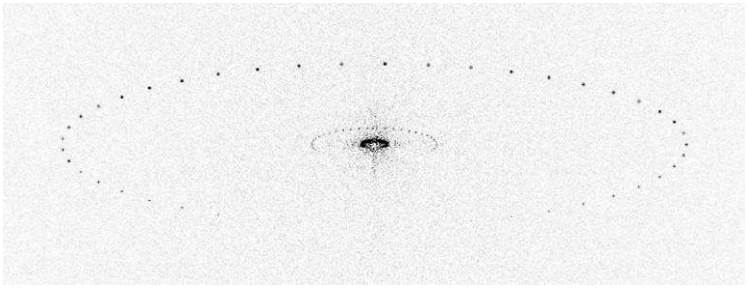

Fig 2. PSF-subtracted, 10^5 sec exposure with OWL of a solar system analogue at 10pc. A Jupiter and an Earth have been put at several positions in their 15^o- obliquity orbit in order to illustrate the phase effect (Hainaut et al, 2004).

120 times longer than OWL to detect the same object. Our simulations [21] indicate that for a solar system analogue at 10 parsec (30 light years) the earth would be detected in about one hour with OWL, opening up the possibility of doing spectroscopy for D > 80m. A recent study by Angel (2003) confirmed that spectroscopy of exo-earths is within the reach of a 100-m in the optical/near-IR, while in the thermal infrared space interferometers (*à la* Darwin/TPF) are moderately better unless the 100-m is placed in Antarctica. Sophisticated coronagraphic techniques, able to suppress by factors upward of 10^6 the light of the parent star may allow to resolve closer separations, at the same time expanding the accessible volume and decreasing the necessary exposure times.

Measure of cosmological parameters with *primary* distance indicators (note: H, not H-not!) Beyond the local universe, distances are determined today using derived standard candles (e.g. SNe Ia) whose calibration is not always completely reliable. OWL will allow the measurement of distances using primary indicators in the redshift range where the difference between cosmological models is more pronounced. Using Cepheids and Novae, as well as the planetary nebulae and globular clusters luminosity functions, accurate measurements of distances can be obtained out to z ~ 1 and these will allow to disentangle the various models, including those alternative to Λ. Beyond z ~ 1, Type Ia SNe can be detected up to z ~ 5 (although Ia's are the second brightest explosions in he universe after GRBs they do not emit in the UV and K being the last useful band they are not detected beyond that z), core-collapse SNe out to z ~ 10, and alleged Pop III SNe even beyond. While SNe may be more useful to determine the cosmic supernova rate, and from this the early universe star formation history, than in disentangling cosmologies, they will provide critical cosmological information up to redshift ~ 10 (e.g. quintessence).

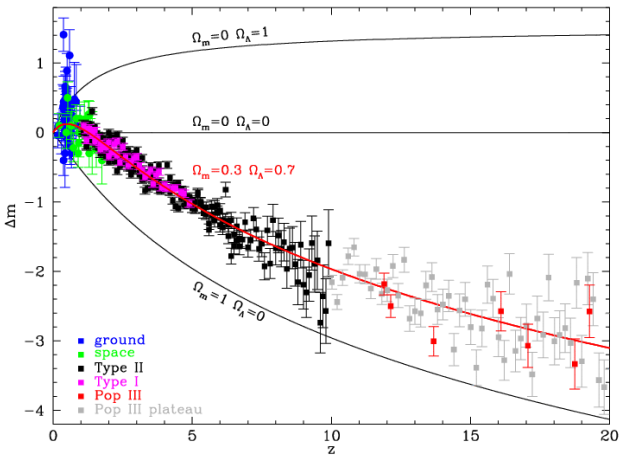

Fig 3. Simulation of OWL observation of supernovae to redshift 20 (Della Valle et al, 2004)

Primordial stellar populations. WMAP sets the recombination epoch at z between 10 and 20. Pop III stars are strong candidates as possible re-ionization sources. Pop III stars are hot and massive, and form *before* re-ionization possibly in dwarf-galaxy sized over-densities (10^6-10^7 M⊙). Strong emission lines of H and He, and strong nebular continuum characterize their spectra. Both the continuum and line spectrum can accurately be studied with OWL at high z, thus detecting and characterizing the first-light objects in the Universe. OWL would be about 10 times more efficient than JWST for these observations.

3. OPTO-MECHANICAL DESIGN

The optical design of OWL [5] is based on a 6-mirror solution, with spherical primary, flat secondary, and a four-elements corrector. The total field of view is limited by rapidly increasing vignetting beyond 10 arc minutes field diameter. The optical quality is fully seeing-limited on the curved field, with 2 arc minutes diffraction-limited in the visible.

This design solution is supported by a number of trade-offs and analysis' [6,7,8]. Reasons for selecting a spherical primary mirror fall in three categories: system reasons, performance aspects, costs and risks.

Compared to a classical 2-mirror design, the 6-mirror one offers a much larger usable field of view, a manageable field curvature, a low sensitivity to (flat) secondary mirror decenters, and excellent baffling options. It allows all wavefront control functions, including dual conjugate adaptive optics, to be eventually realized with no more than 6 surfaces, the last two mirrors of the corrector being conjugated to 8 km and ground, respectively. Finally, a Ritchey-Chrétien solution implies either a 2- to 3-m class secondary mirror, with horrendous centering tolerances, or a very large one (~8-m), whose feasibility is doubtful at best. The comparison is however unfair; the most

realistic aspheric alternative to the current design is probably an on-axis folded Gregorian with flat secondary, whereby a large concave, aspherical mirror would replace the corrector in the current OWL design. The instrumentation would have to be rather inconveniently located behind the secondary mirror.

All-identical spherical segments imply substantial relaxation of fabrication and operation constraints –a non-trivial issue with about 3,000 segments, which need to be produced at a rate of about one per day and re-coated at a rate of about 5 per day. The required number of spares is also lower than with an aspherical design. The spherical shape allows for extensive use of large, stiff polishing tools. Not only do large tools allow for an intrinsically higher productivity than small ones, they are also inherently more performing in terms of high spatial frequency misfigure, most notably rolled edges. An elegant alternative is to stressed polishing, whereby the segments would be polished spherical and attain the desired shape upon relaxation of a dedicated warping harness. Doing so, however, constraints the acceptable residual stresses in the segments blanks, introduces an element of risk, and probably prohibits the use of lightweight, structured segments, e.g. in silicon carbide.

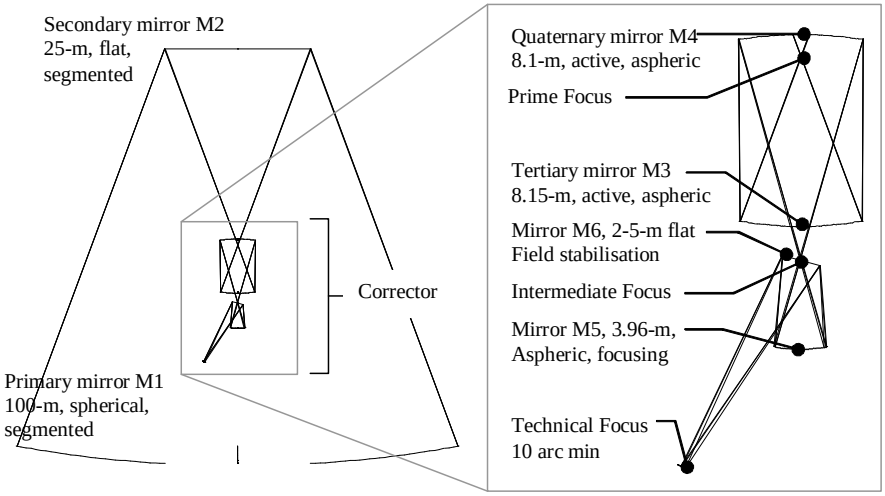

Fig. 4. Layout of OWL optical design

Finally, optical testing of the segments is an integral part of the *serial* fabrication process, and existing solutions for off-axis aspherical segments are not convincingly adequate. Testing of all-identical, spherical segments against a unique, stable matrix seems to be the safest approach to ensuring that tight matching requirements are met.

Still, aspherical segments are most probably feasible, and, allowing for a longer schedule and a yet to be determined optical test strategy, the implied costs and risks, although difficult to predict, might be manageable. The essential point is that an RC or folded Gregorian would fail to meet system and performance requirements –except, perhaps, for seeing-limited or single-conjugate, small field of view modes, and assuming a very large adaptive secondary or tertiary, with commensurate amplitude and dynamic ranges.

The corrector includes two 8-m class active mirrors M3 and M4, the latter highly aspherical and conjugated to the entrance pupil, the former moderately aspherical. A fabrication test setup has been proposed [9], which guarantees the matching of these two mirrors, but the practical implementation of this setup in factory conditions still needs to be reviewed by expert suppliers. The last two mirrors M5 and M6 of the corrector are concave aspherical and flat, respectively, with diameters of 4 and 2.4-m. The implementation plan foresees provisional M5 and M6 units, for on-sky commissioning, to be subsequently replaced by large adaptive mirrors conjugated to 0 and 8km altitudes. The flat M6 can be rotated about the telescope axis to feed any of the 6 focal stations. A significant drawback of the design is the limited design volume available for mirror M6, which much encompass the adaptive support and the tip-tilt mount.

The design is driven not only by optical considerations (optical quality, fabrication aspects) but also by structural ones. Centering has been the plague of classical designs until conveniently remedied by way of closed-loop active optics. Active centering is still mandatory with OWL, but the distribution of tolerances amongst individual surfaces matches ideally what physical constraints allow. Tolerances are most generous where they are most difficult to achieve: lateral decenters of the flat secondary are innocuous, the effect of its tip-tilt is limited and can be fully compensated by a rotation of the corrector about the secondary mirror vertex. The design of the structure relying on parallelogram-shaped modules, lateral motion under load is favored over tilt. Centering tolerances for the corrector are tighter (typically 1 mm and a few arc seconds) but it is favorably located in terms of structural rigidity. Centering tolerances within the corrector are in the sub-mm range, but sensitivities are such that equal movements of the two 8-m mirrors nearly compensate each other's effect on image quality. A sensitivity analysis shows that two of the corrector aspherical surfaces will have to be actively re-centered on the basis of measurements provided by wavefront sensors located at the telescope focus.

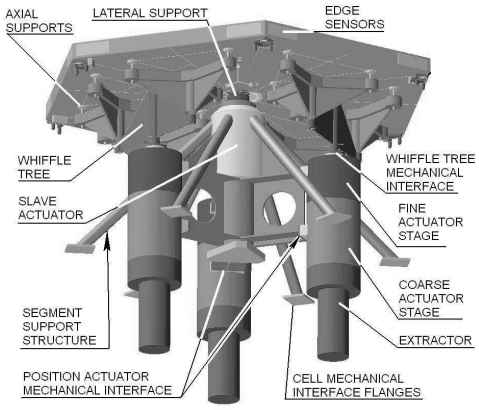

Fig. 5. Segment support system.

The f/1.25 primary mirror is made of 3048 segments, the flat secondary of 216. The 1.6-m flat-to-flat, 70-mm thick, ~400 kg glass-ceramic segments are axially supported by an 18-points whiffle-tree and laterally by a central support (Fig. 5). Quilting under gravity is about 30 nm RMS surface. Assuming that segments will be polished on support systems identical to that in the telescope, this deformation would appear only at high zenithal distance for the primary mirror segments. For the secondary mirror ones, the corresponding spatial frequency, as projected onto the pupil, is about three times lower and could, therefore, be compensated by a suitable offset of the adaptive mirror (M6). Alternatively, the quilting could be polished out for z=0, with the secondary mirror segments optically tested face down.

The two-stage actuators are specified at 60 Hz first eigenfrequency. The coarse stage is specified at ±20 mm stroke and ±50 μm accuracy, the fine stage at ±0.5 mm and ±5 nm, respectively.

The design of the telescope structure (Fig. 6) has been the subject of a major iteration [10], with the initial four-fold symmetry being replaced by a six-fold one. This allows for a near-circular outer rim, and a structural geometry matching that of the segments. As a result, major dimensions are integer multiple of that of the 1.6-m flat-to-flat size of the segments, thereby simplifying interfaces, integration, and allowing for ideal propagation of loads from segments to substructures, structures, kinematics, and eventually foundations. The aptly named *fractal design* relies extensively on standard parts, with about 80% of the moving mass made of standard steel pipes, the rest being mostly made of serially-produced nodes. Fig. 7 shows the basic structural module. Nodes themselves are assembled from no more than 3 types of parts (Fig. 8). Openings allow for unobstructed air flow through the nodes, thereby reducing the thermal time constant. All parts fit into standard containers, modules being assembled on-site prior to integration.

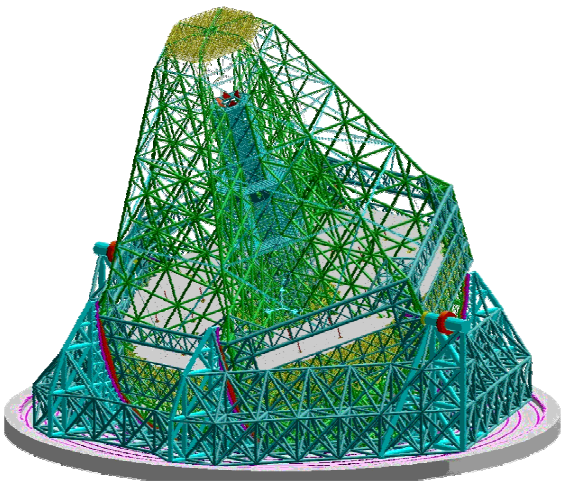

Fig. 6. OWL telescope structure.

The structure is essentially made of mild steel, except for composite tensioning cables, and is designed to withstand middle-range seismicity (0.2g). The total moving mass is 14,800 metric tons, including solid glass-ceramic segments. This figure includes a 90 tons allocation for instruments (15 tons each) and a 500 tons contingency for cables, paint, lifts, etc. The locked rotor eigenfrequency is 2.6 Hz. Table 2 gives the primary and secondary mirror decenters under gravity between zenith and z=60°. The results are deemed excellent for a structure of OWL size, and represent a very significant improvement with respect to the already impressive figures obtained with the former design iteration [6]. The secondary mirror being flat, its lateral decenter is of no consequence. Extensive analyses of the design are presented elsewhere [10]. These analyses rely on detailed Finite Element models including segments supports as well as friction drives.

Mirror	Piston [mm]	Tilt [arcsec]	Decenter [mm]
Rigid body motion, zenith to 60°.			
M1	-7.8	0.1	**-13.2**
M2	-11.2	-2.0	-30.8
M2 – M1	**-3.4**	**-2.1**	-17.6
Peak-to-valley motion, zenith to 60°			
M1	**10.1**	**147.1**	**8.8**
M2	2.8	132.7	1.1

Table 2. Displacement under gravity

The kinematics is provided by friction drives, the elevation structures "rolling" on 2 cradles, the azimuthal ones on tracks embedded into the foundations. This solution has been selected against hydraulic pads and tracks, which would imply very high costs and unrealistic dimensional tolerances over very large scales. A control model is being assembled [10], under contract with the *Technische Universität München* and *Ecole Polytechnique Fédérale de Lausanne*. A breadboard is also foreseen as part of a technology development proposal submitted to the European Commission within Framework Programme 6.

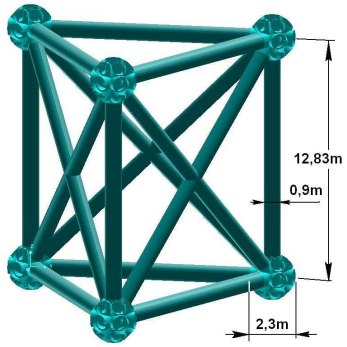

Fig. 7. Basic structural module.

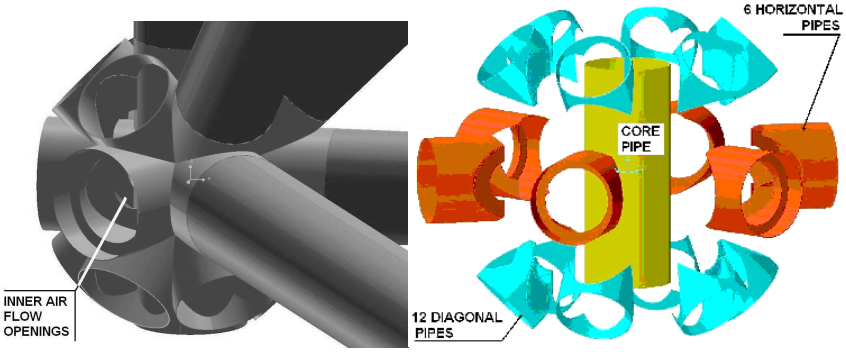

Fig. 8. Structure node.

The telescope would operate in open air, a sliding enclosure providing shelter during daytime and adverse meteorological conditions. The enclosure is dimensioned to permit full kinematics of the telescope, with a view to allowing integration and maintenance under protected conditions.

4. SEGMENTS FABRICATION

Fabrication of the segments has been addressed in depth by way of industrial studies. Three optional segment sizes have been considered: 1.3, 1.8 (baseline) and 2.3-m flat-to-flat. Contracts for feasibility studies were placed with Zeiss-Lzos, Schott and Corning (Astro-Sital, Zerodur or ULE blanks, respectively), Boostec-Astrium and ECM (Silicon Carbide blanks), Sagem-Reosc and Seso (polishing). With only one exception, these studies gave remarkably consistent results, confirming that delivery of the segments within tolerances and specified time scales – typically, a 6 years production cycle preceded by 2-3 years setting up of the production lines- and at a cost roughly in-line (within less than 20% at worst) with ESO's initial estimate. All studies point towards higher complexity and cost for the largest size (2.3-m), the optimal size being the intermediate one (1.8-m) or slightly smaller. The consistency of the results is attributed to the fact that the dimensions and spherical shape of the

segments are compatible with fully qualified tools and processes –except for the largest size, which is no longer considered as an option.

These studies generally assumed conservative yields of individual processes, and capital investments (e.g. number of machines) were defined accordingly. For example, it was assumed that all segments would have to undergo optical finishing with either computer-controlled, small tool or ion-beam techniques. In practice, a fraction of the total production will probably meet specifications without the need for small tool finishing.

Both optical manufacturers (Sagem-Reosc and Seso) identified several possible figuring strategies, all relying on proven processes and tooling (except for the largest size). Matching the tight rolled edge specification is an issue that must be tackled with in the earliest stages of processing. The spherical shape of the segments is favorable in that it permits the use of full-sized, stiff tools. Those allow for faster figuring (in proportion to the tool area), smoother surface, and lower rolled edges. All segments can be tested against a unique reference matrix, thereby ensuring proper matching of the individual segment's curvature. A spare matrix is evidently required for safety reasons, but the latter can be correlated with the master one by testing against a common reference segment.

Front-back CTE or thermal gradients being a potentially serious issue, the optical manufacturer is nominally required to optically test the segments at the expected median temperature (5 ^{o}C) in operation. Figuring itself can of course be performed at factory temperature. Although not a major issue in serial production, where batches of segments can be queued for cooling without disruption of the global yield, it implies additional complexity and investments. There is reasonable hope that measurements on pre-production segments would allow dropping this requirement, and having it replaced by periodic verification on subsets of segments. In the absence of a database of accurate measurements of typical blanks front-to-back CTE gradients, we cautiously assume that cold optical testing will be required.

Fig. 9. Boostec SiC prototype segment blank.

As of today, the baseline material is low-expansion glass-ceramics, for its proven characteristics. The option of silicon carbide is however vigorously pursued. With much higher specific stiffness, low coefficient of thermal expansion, and excellent thermal conductivity, this material would allow for superior performance. Silicon carbide mirrors, however, tend normally to be far more costly than low-expansion glass ones, but this is mostly due to the fact that they are relied on for space applications, where mass requirements drive the technology to its limits. With OWL, suppliers have been given the freedom to set the mass requirement to what their processes and tooling could most efficiently do, the upper limit being tentatively set at 70 kg/m². As a result, suppliers came with similar, simple segments designs compatible with serial production at attractive costs. Owing to its excellent machinability in the early stages of forming, to the possibility of assembling pre-machined parts prior to firing without subsequent deterioration of the final optical surface, to the fast cold-to-cold ceramization, and to predictable dimensional changes (if any), raw silicon carbide blanks would, according to suppliers, be at a cost advantage with respect to classical glass-ceramics. This advantage is somewhat lost in the very high costs of overcoatings and polishing as all types of silicon carbide substrates investigated so far require such hard overcoatings for pore-free, low microroughness (~20Å) optical surface. Possible overcoatings include Chemical Vapor Deposition (e.g. Schunk CVD) or Isothermal Chemical Vapor Infiltration (e.g. Snecma ICVI). A major issue is that the polishable overcoatings may lead to differential bimetallic effects between individual segments, thereby ruling out the technology. There is, however, growing evidence pointing to the contrary. Attractive alternatives, whereby low microroughness would be provided through a thin (~10 μm) overcoating deposited at the final stage of

polishing, have been proposed as well. The silicon carbide option and underlying technologies will be evaluated by optical manufacturers within the framework of a forthcoming European technology development programme for Extremely Large Telescopes. Four segment prototype blanks, 1-m flat-to-flat, have been supplied by Boostec for testing (Fig. 9), up to four more will be supplied by ECM in 2005. Final test results are expected by 2006.

At project level, the total cost impact of silicon carbide is yet unclear. A preliminary design analysis shows that the savings on the total moving mass could be on the order of 5,000 tons; consequences at the level of segments supports and position actuators still need to be quantitatively assessed. It is also expected that lightweight segments would translate into increased telescope stiffness and bandwidth of the closed loop phasing, thereby improving performance under wind excitation.

It should be noted, finally, that recently SCHOTT invested in a Zerodur production capacity comparable to the one it had foreseen in its OWL segments feasibility study. Although aimed at a different market, the investments are reportedly in-line with those expected for OWL. In addition, Schott claims cost improvements in the casting process, and that cost-effective 50% lightweighting of segments blanks might be possible; definite numbers are, however, not available at the time of writing of this article.

Meanwhile, the baseline segment characteristics have been reduced to 1.6-m flat-to-flat, 70-mm thick solid glass-ceramics, all-identical hexagons. This should lead to a slight cost reduction for the segments, and 1.6-m is probably the largest size where an 18-points axial support could still meet specifications. Another reason for the segment's size is the integer ratio between the latter and the size of the basic structural module, itself being dimensioned by the dimensions of standard transport container. This integer ratio is at the core of the structure's *fractal* design, with its optimal standardization of opto-mechanical interfaces and ideal propagation of loads.

5. WAVEFRONT CONTROL

The term *wavefront control* covers all functions required for the telescope to provide a properly guided, stable image, ideally free of residual aberrations. We distinguish 5 essential types of functions (table 3).

Type	**Max. expected frequency**	**Drive / Active element / Degree of freedom**	**Metrology**
Pre-setting	~0.1 Hz	Corrector kinematics, M4 & M5 centering, M5 refocus, M6 tip-tilt mount	Fiber extensometer or equivalent; load sensors on active mirrors.
Tracking			
Guiding	~0.5 Hz	Telescope drives	Guide probes
Field stabilization	~5-10 Hz	M6 (tip-tilt mount)	Guide probes
Active optics			
Deformable mirrors	1 (goal 5) Hz	M4 (8-m active deformable mirror)	Active optics wavefront sensors
	1 Hz	M3 (8-m active deformable mirror)	Idem
Active centering	0.1 Hz	Corrector kinematics	Idem
(coma correction)	0.5 Hz	M4 centering	Idem
	5-10 Hz	M5 centering	Idem
Active focusing	1 (goal 5) Hz	M5 focusing	Idem
Phasing			
Closed loop	3 (goal 5) Hz	M1 and M2 segments (position actuators)	Edge sensors
Calibration	N/A	M1 and M2 segments (position actuators)	Phasing wavefront sensor
Adaptive optics			
Seeing reduction	~100 Hz	M6 adaptive unit	Adaptive optics wavefront sensors
Single conjugate IR	~100 Hz	M6 adaptive unit	Adaptive optics wavefront sensor
Dual conjugate IR	~100 Hz	M5 and M6 adaptive units	Adaptive optics wavefront sensors
Visible AO	> 100 Hz	M5 and / or M6 adaptive units + post-focus corrector	Adaptive optics wavefront sensor(s)

Table 3. OWL Wavefront Control functions.

Pre-setting is aimed at guaranteeing that a sky reference can be effectively acquired by the guide probes and active optics wavefront sensors. In practice, this implies collimation and image quality in the arc second range, i.e. relocation of the corrector and of selected surfaces within the corrector to typically 10 ppm of linear distances, and

force settings of the 8-m active mirrors to an accuracy comparable to that of the VLT primary mirror load sensors. All this, however, relies on the assumption that initial integration procedure can be performed to compatible accuracy, which remains to be established.

Preliminary analyses indicate that the telescope kinematics should be able to point and track to sub-arc second accuracy [10]. Field stabilization is required to compensate for the effect of wind on the primary and secondary mirrors, and to a lesser extent on the corrector. It is assumed that the adaptive M6 unit, coinciding with the exit pupil, will be mounted on a dedicated tip-tilt mount, with a sky amplitude on the order of 2 arc seconds. As the required bandwidth overlaps with that of atmospheric tilt, and conservatively assuming an infinite outer scale, several guiding probes are required to disentangle the effect of atmospheric turbulence from the telescope tracking errors.

The OWL active optics concept differs only incrementally from that of the VLT. Its essential purpose is to relax optical fabrication tolerances (mirrors of the corrector) and compensate for slowly varying alignment errors. Coarse focusing is provided by the corrector kinematics, fine focusing is done by axial translation of the mirror M5. The two deformable 8-m mirrors, M3 and M4, are similar to the VLT primary mirrors and require comparable supports – the essential change being that M4 is operated face down. M4 coincides with a pupil, M3 is conjugated to about 2.4 km altitude. The dual conjugation of the active mirrors requires several references to disentangle in-pupil aberrations from field dependent ones. In theory, three wavefront sensors would suffice; in practice, we assume that 5 to 7 wavefront sensors will be required to accommodate for possibly unfavourable distribution of reference sources in the field of view. In-pupil wavefront sensing (Pyramid or curvature) is preferred over Shack-Hartmann, to allow flexibility with sampling. Compensation of large scale deflections of the primary mirror up to ~1 Hz with M4 is an option that remains to be investigated. The main issue is not the active mirror per se – the VLT primary mirrors are dimensioned for open loop correction up to 1 Hz- but the cross-talk with ground layer turbulence.

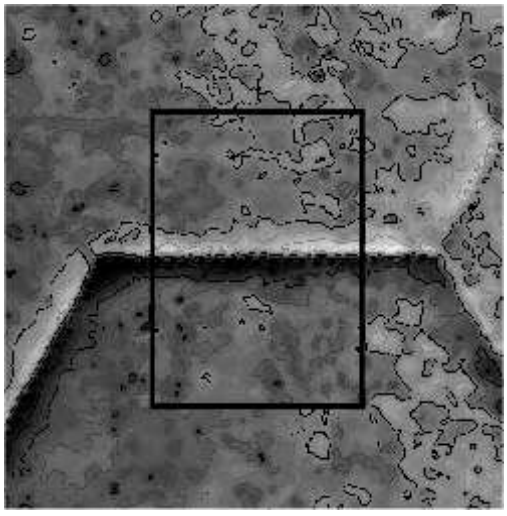

Fig. 10. Laboratory interferogram of a segmented phase screen through a Mach-Zehnder phasing sensor.

The primary and secondary mirrors are phased independently, the signal being provided by sensors located at the inter-segment edges. The baseline solution relies on capacitive sensors; *Fogale Nanotech* is currently working on an evolution of the technology it implemented in the South African Large Telescope. Three possible on-sky calibration techniques are currently under development by various European institutes. Diffraction Image Phase Step Sensing (DIPSS) is being developed at IAC and GRANTECAN by Schumacher et al [3] and holds the promise of spectacularly simple hardware requirements. Laboratory tests gave a typical accuracy of 15 and 25 nm wavefront RMS, without and with turbulence generator (0.6 arc seconds seeing), respectively. Esposito et al [2] have shown that pyramid wavefront sensors could deliver the piston and tip-tilt measurements. At LAM and ESO, Montoya, Dohlen and Yaitskova [4] made extensive modeling of a Mach-Zehnder phasing sensor, and laboratory tests have started (Fig. 10). It has been shown [6] that Fourier filtering allows to disentangle the signals associated to individual segmented surfaces. We conservatively assume that calibration will have to be performed on seeing-limited images. Relative seeing-independence require long exposures or adequate filtering –e.g. by adjusting the size of the spatial filter in a Mach-Zehnder phasing sensor. In practice, feedback from the adaptive optics metrology will most likely be possible but, at this stage, cannot be exclusively relied on.

All three techniques will be evaluated on-sky. A technical instrument –APE for *Active Phasing Experiment*- is in the conceptual design phase [11]. It will be mounted on a VLT unit telescope, with results expected in 2007. APE is essentially a pupil re-imager, with a segmented mirror conjugated to the VLT primary mirror, feeding an array of

phasing sensors. In addition to allowing real-time comparison of each sensing technique, it will serve as a breadboard for the integration of a segmented aperture in an active telescope.

Metrology requirements underlying the wavefront control functions imply quite a number of guide and wavefront sensing probes –indeed the sky area covered by wavefront sensors may at least occasionally exceed that of the science instrument. Non-adaptive functions do not *a priori* require on-sky sensing close to the science target(s), can accommodate relatively long exposure times and low pupil sampling. We expect the arrays of non-adaptive on-sky sensors at each of the 6 foci to encompass:

1. Up to 5 full-aperture guiding sensors, with exposure times of at least 10 ms, for guiding and field stabilisation.
2. 5 to 7 active optics wavefront sensors, with exposure times of at least 20 ms, for active optics functions.
3. At least 1 phasing wavefront sensor, for occasional (at least once per night) calibration of the position sensors.

Note that the guide probes and active optics sensors can, as in the VLT, rely on the same sources. Guide probes, active optics and phasing wavefront sensors shall à priori rely on references located outside the adaptive optics control field, conservatively set to 6 arc minutes in diameter. At worst, this still leaves about ½ of the total accessible field area for non-adaptive wavefront control. A detailed assessment of the implied sky coverage still needs to be done, but subpupil size and/or exposure times are such that sky coverage is expected to near 100%. In the future, active optics and phasing metrology may presumably evolve into a global concept relying on identical hardware but different data processing.

Of crucial importance for the performance of the telescope and the dimensioning of its control systems is the effect of wind on the telescope structure and optics. The issue is one of amplitude *and* frequency, quasi-static effects being generally much easier to cope with and high frequency pressure turbulence being the most undesirable. By design, OWL is insensitive to lateral M1-M2 decenters, and the parallelogram-shaped structural modules tend to naturally favour lateral decenters over tilt. The structure being mostly exposed to laminar wind flow, image motion is essentially quasi-static and within the correction range of field stabilization with M6 [10].

The effect of dynamic wind pressure on the primary and secondary mirrors is far more difficult to assess. Computational Fluid Dynamics (CFD) models provided very optimistic results but there is strong suspicion that beyond ~0.5 Hz those analyses failed to sample high frequencies adequately –even with ~20 million voxels models. Wind tunnel testing may seem to be the most obvious solution, but sampling limitations and inaccurate scaling laws may lead to the same pitfalls as CFD analysis, thereby giving a fake impression of consistency between similarly flawed results. Representative measurements are better, and currently implemented on the Lovell radio-telescope, thanks to the cooperative spirit of Jodrell Banks Observatory. First measurements are expected to take place in August 2004.

We expect to correct for the effect of wind by combining active deformations (active optics) of M4 -for large amplitude, low spatial hence temporal frequency modes- with active re-positioning (active segmentation) of segments for high frequencies, low amplitude modes. This strategy owes to the inherent properties of each control system, active optics being most efficient on low and active segmentation on high spatial frequencies. This includes metrology considerations, with active optics relying on wavefront sensors and active segmentation on fast position sensors.

Measurements, models and feasibility studies for the implied hardware are still required to confirm currently encouraging but inaccurate assessments. Several options could be implemented to mitigate the effect of wind, if required. This includes

- Installing louvers in the azimuth structure, thereby shielding the primary mirror up to $z \sim 30^{o}$;
- Increasing local stiffness of the segments supports (currently specified at 60 Hz);
- Increasing the bandwidth of the M1 control system (currently specified at 5 Hz), lightweight segments would, in this respect, be an advantage;

- Setting operational constraints i.e. restricting wavelength to IR with high (~8-10 m/s and above) ground wind speed. It should be noted that *this restriction is likely to apply anyway*, as the performance of AO system degrades with faster ground turbulence.

Relying on adaptive optics for low- and mid-spatial frequency disturbances is another option; this may however imply undesirable constraints on the adaptive mirror technology.

Adaptive Optics (AO) is widely recognized as the most daring challenge. The OWL implementation plan is, to a large extent, optimized to allow progressive implementation of increasingly complex adaptive systems, and to relax schedule pressure on technology development.

The objective for the first adaptive system is to deliver NAOS-type performance with a 60-m filled aperture, and is due to enter science operation by end 2016. The plan is to mount a provisional M5 unit that will re-image the 60-m entrance pupil onto the 2-m class adaptive M6. The implied actuator interspacing requirement for M6 is ~20 mm, with a goal of 15-mm as the unit will be eventually operated with the full 100-m aperture. Compared to current LBT technology this implies, roughly, a factor 2 increase in corrector size and in actuator density –an ambitious but not unreasonable step over 10 years. Would the increase of monolithic shell size and actuator density lead to insurmountable challenges, a segmented M6 with 6 petals, each about 80-cm in length, matching the pupil obscuration and geometry, and mounted on piezo stacks, is considered as a backup. M6 being conjugated to ground, can in principle deliver Single Conjugate AO or wide-field seeing reduction.

The second system, to come into operation with a ~80-m filled aperture, is dual-conjugate IR AO, the provisional M5 unit being replaced by the final, 3.5-m AO one. Owing to its larger diameter and –at worst- identical actuator linear density, this unit should permit either higher order correction or, in multi-conjugate mode, wider field IR AO correction. On the negative side, this will imply a lower sampling of the ground layer, the M6 being by then used in its final configuration as a 100-m conjugate.

For high order correction, due to come into operation at the latest stages of integration, the above systems shall serve as first stage, low-order, large amplitude correctors. Unless the progress of technology would permit that the M6 be upgraded to very high actuator density (~3-5 mm actuator interspacing), visible AO will have to rely on post-focus AO / Multi-Conjugate AO (MCAO) correctors, most probably based on MEMs technology. At visible wavelengths, acceptable sky coverage will require multiple Laser Guide Stars, and suitable approaches to dealing not only with elongation and cone effect, but also with the inherently poor performance of a telescope the size of OWL in re-imaging references at finite distance [7].

Two different single conjugate Single Conjugate AO (SCAO) systems for OWL have been simulated. The first one uses a Shack-Hartmann (SH) sensor and the second a Pyramid wavefront sensor (Pyr). Both systems used the same deformable mirror (DM). The goal of this study was to get a crude performance estimate and to compare the two wavefront sensing schemes. Also, two telescope diameters (60m and 100m) were investigated, following the concept of growing a telescope. In both cases, the same number of actuators and sub-apertures were used. This means that the 60m case has a higher actuator density, and provides a higher Strehl, at the cost of lower angular resolution. Underlying this assumption is the provision that, in the first stages of operation, a temporary M5 pupil re-imaging unit will be integrated into the telescope, so as to use the full aperture of the M6 mirror even though the telescope pupil is not entirely filled.

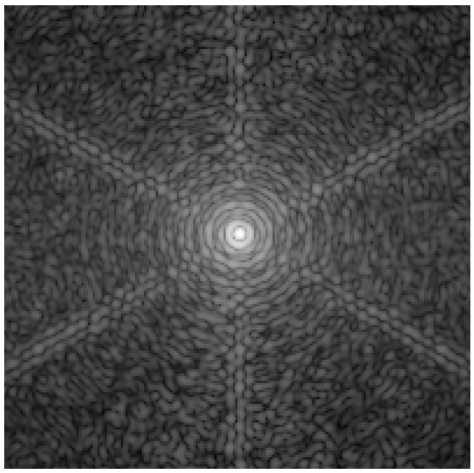

Fig. 11. Simulated OWL PSF under 0.5 arc seconds seeing, with bright guide star, K band, taking into account residual atmospheric and segmentation errors. Logarithmic scale. Strehl is 70%.

The models used the following parameters:

- 125 sub-pupils across the aperture
- Very bright on-axis single natural guide star
- Single deformable mirror conjugated to the ground
- Central obstruction 35% linear
- Scientific imaging wavelengths from 1.25 μm to 10 μm
- Segmentation errors, pupil shape and spiders taken into account

Fig. 11 shows the simulated PSF (100-m telescope) with the SH system. The image is 0.3" on a side. The diffraction limited core (the Strehl Ratio is ~70% at K-Band, on-axis) and the structure created by the obscuration are clearly visible. The stretch is logarithmic.

The main difficulty in this study was the sensitivity of the pyramid sensor to the large central obstruction. As a result, some actuators near the central obstruction were not controlled properly. This can certainly be solved by a combination of modulation in the calibration phase (which was not done here, because it is very computing time intensive) and a more elaborate control algorithm. Otherwise, both sensors produced very similar results. A more thorough comparison of SH vs. Pyr, including early results of a possible Ground Layer AO system for OWL, is presented elsewhere by Le Louarn et al. [12].

MCAO concepts will be verified by 2005 in the laboratory and on-sky with the Multi-conjugate Adaptive optics Demonstrator, currently under construction [13].

6. SITE CHARACTERIZATION

The OWL site shall provide the optimum operating conditions, not only in terms of sky transparency but also for the performance of adaptive optics atmospheric correction. The latter sets the requirements for the development of a new generation of site testing instruments providing the detailed vertical profile of the turbulence. These new profilers such as MASS [14] and SLODAR [15] are currently deployed on the existing observatories of VLT at Paranal and ORM at La Palma. The list of pertinent characteristics is not limited to atmospheric turbulence but must also include diverse parameters such as water vapor content, soil properties, light pollution, topology, access to existing infrastructure, potential environmental restrictions, etc.

Simultaneously, new sites are being explored in North-West Argentina, potentially less seismic than the Chilean coast, and in Morocco where seeing measurement started [16] and the effect of desert aerosol on atmospheric extinction has been investigated [17]. These new sites are to be later equipped with portable versions of the above mentioned turbulence profilers.

The long term climatic trends of all candidate sites will be thoroughly studied by means of a web-based tool developed for this purpose [18]. Finally, candidate sites shall be compatible with a realistic construction schedule and affordable operational costs.

7. INSTRUMENTATION

The major science drivers for an OWL class telescope fall in three outstanding –and extremely challenging- domains: imaging and characterization of exo-solar planets down to earth-like objects; probing of the early Universe in particular from very high z Supernovae and possibly from Population III clusters; photometry of individual stars in external galaxies and in particular in giant Elliptical galaxies.

Translated into instrumental requirements, the first science driver requires extreme contrast (but not necessarily extreme Strehl) AO in the near IR, preferably the J & H bands [19]. The second one requires dual conjugate AO in the near-IR (up and in particular in the K-band) with full diffraction-limited sampling for imaging and a significantly coarser sampling for (multi integral field units) spectroscopy. The last one calls again for dual conjugate AO and full diffraction-limited sampling. Working in the near-IR would be a good first step there; however getting the full astrophysical potential ultimately requires observing in visible wavelengths. The two last science drivers do require in addition a high sky coverage which could indeed be provided by OWL for reasonable atmospheric conditions in K and exceptional ones in J. Of course, this is not a problem in the case of the first driver for which the central star provides a strong enough (actually too strong!) beacon.

Fig. 12. A small section of the HST Ultra-Deep Field. Spectroscopy of the faintest galaxies in such images is one primary goal of an Extremely Large Telescope.

It is quite comforting that the AO implementation strategy presented herein, and largely based on technological availability, matches relatively closely these scientifically-based requirements. The post-AO instrumentation, in terms of physical scale and metrological accuracy, would be actually quite similar to corresponding so-called VLT 2nd generation instruments presently under development: the Planet Finder for the exo-solar planets science case; KMOS for the early Universe spectroscopy; the VISTA IR camera for the early Universe imaging and the first step towards resolving external galaxies into stars. As with Planet Finder, but unlike KMOS and VISTA IRCAM, OWL AO sensing should be fully integrated inside the instruments.

In conclusion, the good news is that the challenging but not unreasonable AO strategy presented above does match quite closely the major science drivers for OWL and that the corresponding instruments belong to the same class as instruments presently being developed for 8-10 m telescopes. Two caveats are needed here: all OWL instruments should be very closely integrated with their AO systems, which themselves do scale steeply with the telescope diameter.

8. OPERATION CONCEPT

The technical and scientific operations of OWL are expected to significantly differ from past experiences within the astronomical community. This in itself is not new territory as the current generation of 8-m class facilities is already operating significantly different paradigms than classical observatories of the previous generations, and upcoming large, unique facilities like ALMA will enforce further evolution of such paradigms.

The integration of a detailed operation concept study at the conceptual design phase aims at an early identification of aspects that are critical to the technical and scientific operations of an Extremely Large Telescope, and devise operations schemes that ensure the optimal exploitation of scientific capabilities of the telescope and instrumentation. These aspects are expected to generate level one technical requirement driven mainly by astronomical goals.

Some of the most outstanding technical issues relate to the operation of the telescope in continuous adaptive optics closed loop. These include the modeling of the point-spread function across the field of view, the requirements on pointing, guiding, and tracking, the determination of vibration limits, and the constraints on chopping and nodding that are fundamental for the operation of the associated infrared instrumentation. Also essential for the performance of the instrumentation are the emissivity specifications of the telescope and the pupil stability. The open-loop performance of the telescope, such as the effects of alignment errors previous to the closing of the active optics loops on the ability to acquire guide stars, plays a major role in constraining time requirements and strategies for presetting and acquisition. Two other major technical issues to be considered in the framework of both operational and scientific requirements are the effects of atmospheric dispersion and the trade-offs of compensating or not for it, and the time resolution of observations and the subsequent requirements on PSF stability.

Early consideration is given to technical operations and maintenance aspects, defining the metrology parameters needed to predict maintenance needs and estimating the staffing needs for maintenance. An analysis of the drivers of needs in terms of maintenance staff must pay special attention to the identification of technical design aspects that could alleviate such needs and of potential high cost areas.

Finally, the end-to-end science operations paradigm for the facility must be investigated. Technical design options that may affect the ability to pursue certain classes of science programs should be evaluated taking into account both the priorities set by science case drivers, and their implementation cost in terms of human resources. Also to be considered are scheduling principles on the long and short timescales, the model for the interaction of general users with the facility, data distribution policies and Virtual Observatory-readiness of the data products, and guidelines for the construction and integration of instruments built by external consortia.

9. COST AND SCHEDULE ESTIMATES

OWL cost and schedule estimates are still provisional, as further analysis and feasibility studies are required to complete phase A. The total expected cost, including manpower and prototyping in phase B, amounts to 1.2 billion Euros, including a 10% contingency but excluding operational costs of start of science operation with a partially filled aperture. Roughly ½ of the estimated capital investment (940 million Euros) is already supported by competitive industrial studies. Those essentially cover segments fabrication and the telescope structural elements.

The dispersion of competitive supplier's estimates is rather low, typically below 20% (and in crucial areas much less) with comparable subsystems technologies and specifications. This encouraging factor is, to a large extent, attributable to the fact that OWL's non-adaptive subsystems rely extensively on proven, well established technologies and processes. The benefit of serial production and integration has often been underestimated, industrial studies yielding estimates generally below initial expectation.

Further studies are planned until completion of phase A, to consolidate the cost estimate and the conceptual design. At the time being, the largest uncertainty in the current cost figures is related to the foundation, enclosure and infrastructures, which to some extent are site-dependent, to the cost of the most aspheric mirror of the corrector and the cost of the first three instruments, of the segments actuators and position sensors, and to the cost of the adaptive system. 110 million Euros have been allocated to the AO subsystems (capital investment), including ~10 million Euros for prototyping and competitive preliminary designs.

A rather detailed implementation plan has been assembled, assuming a start of phase B in 2006. This phase would incorporate the final design of time-critical subsystems (enclosure, telescope structure and kinematics, segments, corrector, integration facilities), and preliminary designs of uncritical subsystems. The plan is, to some extent, optimized to allow maximum development time for rapidly evolving technologies, mainly adaptive optics. Final site selection is assumed to take place by 2008.

The phase C/D would start in 2010, with large investments quickly ramping up while ESO's investments and resources in ALMA are ramping down. This is the most constraining schedule requirement; to a large extent, earlier groundbreaking would lead to a correspondingly earlier first light.

In the current plan, subsystems on the critical path are the enclosure and the telescope structure and kinematics. Both subsystems being highly modular and relying on either standard or serial production, supply and integration lines could easily be duplicated to accommodate a faster schedule. Structures and shelters of even larger sizes have been integrated two to three times faster in the past, e.g. the SIAT Zeppelin shelter (which could house two OWLs!) erected in two years, or the 19th-century 7,000 tons Eiffel tower, also erected in two years. The shortest timescale between groundbreaking and first light is set by the 8-m mirrors of the corrector; on the basis of the VLT experience we have assumed that these two mirrors could be produced within 6 years.

The plan allows for early start of science operation with a partially filled aperture, thereby taking the segments out of the critical path. The contracts for the production of the segments, as shown in Fig. 13, is actually not planned as early as possible, in order to (partially) reduce cash flow requirements in the early phases of construction. Industrial

estimates concur that the segments could be produced within a 6 years cycle, preceded by 2 years for the setting up of the production line.

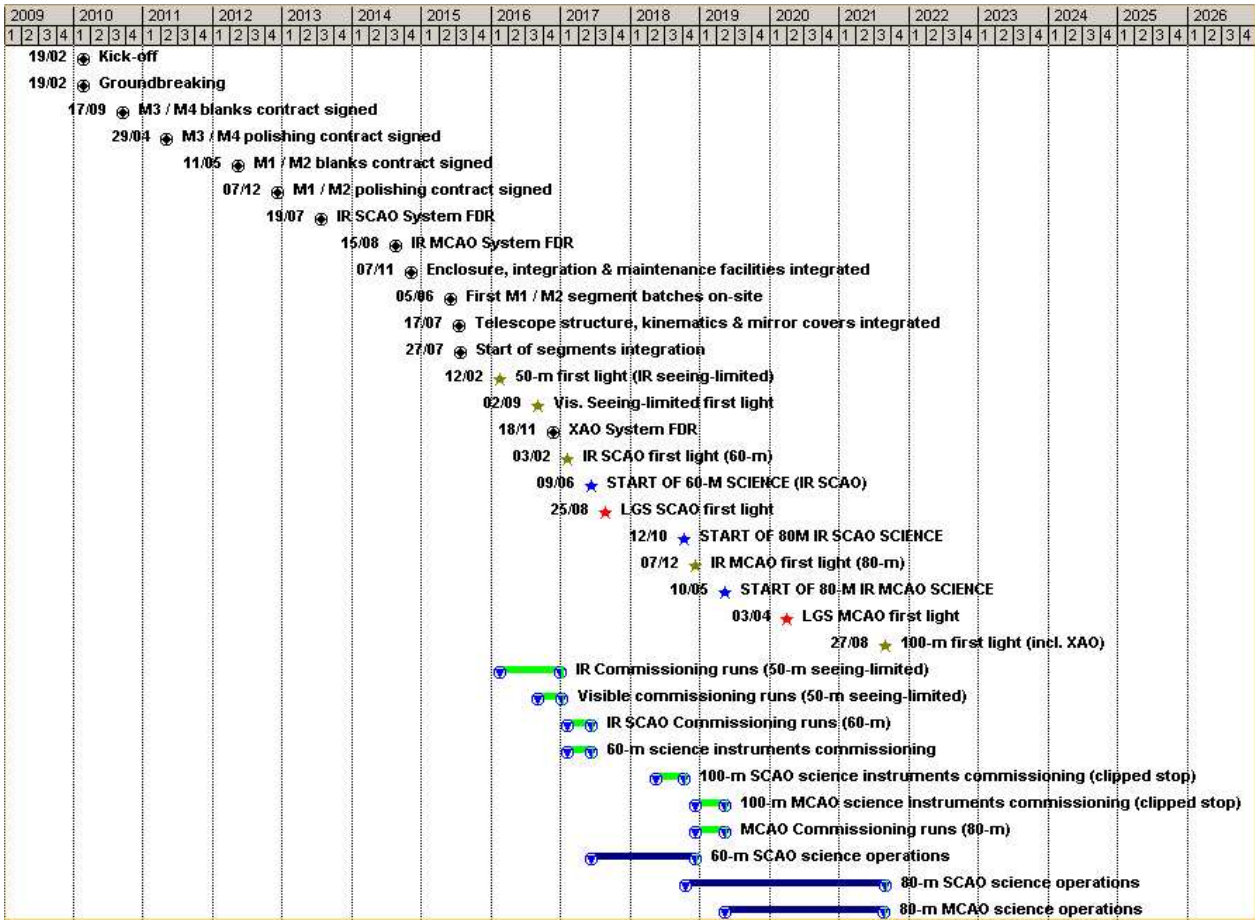

Fig. 13. Major milestones, construction phase.

On this basis, first light would occur in 2015 with a ~30-m equivalent aperture, growing to 50-m in 2016, 60-m in 2017 and eventually 100-m in 2021. Provisional, non-adaptive M5 and M6 units would be installed in 2015 to allow commissioning in seeing-limited mode; we conservatively assume that the telescope would move to science operation in 2017, with a 60-m aperture and single conjugate IR adaptive optics.

REFERENCES

1. R. Gilmozzi, B. Delabre, P. Dierickx, N. Hubin , F. Koch, G. Monnet, M. Quattri, F. Rigaut, R.N. Wilson, *The Future of Filled Aperture Telescopes: is a 100m Feasible?*; 1998, Advanced Technology Optical/IR Telescopes VI, Proc. SPIE **3352**, 778
2. S. Esposito, N. Devaney, *Segmented telescopes co-phasing using Pyramid Sensor*, 2002, ESO Conference and Workshop Proceedings, Vol. 58.
3. A.Schumacher and N.Devaney, *DIPSS: cophasing segmented mirrors with minimal hardware requirements*, 2004, Applied Optics, **in press**.
4. N. Yaitskova et al, "A Mach-Zehnder phasing sensor for extremely large segmented telescopes: Laboratory results and closed loop algorithm," 2004, Proc. SPIE **5498**.
5. E. Brunetto et al, *Progress of ESO's 100-m OWL optical telescope design*, Proc. Bäckaskog Workshop on Extremely Large Telescopes, 2003..

6. P. Dierickx, J. L. Beckers, E. Brunetto, R. Conan, E. Fedrigo, R. Gilmozzi, N. Hubin, F. Koch, M. Le Louarn, E. Marchetti, G. Monnet, L. Noethe, M. Quattri, M. Sarazin, J. Spyromilio, N. Yaitskova, *The Eye of the Beholder: Designing the OWL*, 2002, Proc. SPIE **4840**.
7. P. Dierickx, *Optical design and adaptive optics properties of the OWL 100-m telescope*; Proc. ESO Conf. *Beyond Conventional Adaptive Optics*, 2002, ESO Conference and Workshop Proceedings, Vol. 58..
8. P. Dierickx, B. Delabre, L. Noethe, *OWL optical design, active optics and error budget*; Proc. SPIE, **4003**, 2000.
9. P. Dierickx, R. Gilmozzi, *OWL Concept Overview*; 2000, Proc. Bäckaskog Workshop on Extremely Large Telescopes, p 43.
10. E. Brunetto, M. Dimmler, F.Koch, M Quattri, M.Müller, B.Sedghi, *OWL opto-mechanics, phase A*, Proc. SPIE **5489**, 2004.
11. F. Gonté et al, *APE: a breadboard to evaluate new phasing technologies for a future European Giant Optical Telescope*, Proc. SPIE **5489**, 2004.
12. Le Louarn et al., *Simulations of (MC)AO for a 100-m telescope*, Proc. SPIE **5490**, 2004.
13. E. Marchetti et al, *MAD status report*, Proc. SPIE **5490**, 2004.
14. Kornilov V., Tokovinin A., Voziakova O., Zaitsev A., Shatsky N., Potanin S., Sarazin M., *MASS: a monitor of the vertical turbulence distribution*. Proc. SPIE, V. 4839, p. 837-845, 2003.
15. R. W. Wilson, *SLODAR: measuring optical turbulence altitude with a Shack-Hartmann wavefront sensor*, Mon. Not. R. Astron. Soc. **337**, 103-108, 2002.
16. Z. Benkhaldoun, A. Abahamid, Y. El Azhari and E. Siher, *OWL Site Survey: first seeing measurements with ADIMM*. SPIE 5489-10, June 2004.
17. E. Siher, S. Ortolani, M. Sarazin, Z. Benkhaldoun; *Correlation between TOMS aerosol index and astronomical extinction;* SPIE 5489-13, June 2004.
18. E. Graham, M. Sarazin, M. Beniston, C. Collet, M. Hayoz, M. Neun, S. Goyette; *Site Selection for OWL using past, present and future climate information;* SPIE 5489-12, June 2004.
19. R. Gilmozzi, *Science and Technology Drivers for Future Giant Telescopes*, Proc. SPIE **5489**, 2004.
20. I. M. Hook, *Highlights from the science case for a 50- to 100-m extremely large telescope*, Proc. SPIE **5489**, 2004.
21. O. Hainaut, F. Rahoui, R. Gilmozzi 2004, in proc Berlin conference on "Future Astrophysical Instruments for the 21st century", in press.
22. M. Della Valle, R. Gilmozzi, P. Madau, N. Panagia, 2004, in proc Berlin conference on "Future Astrophysical Instruments for the 21st century", in press.